# Using Fuzzy Structural Information for the Recognition of Cerebral Structures

Thierry Géraud,* Isabelle Bloch and Henri Maître

*Ecole Nationale Supérieure des Télécommunications – Département TSI, CNRS URA 820*
*46 rue Barrault, 75013 Paris, France – Tel: +33 1 45 81 75 85, Fax: +33 1 45 81 37 94*
E-mail: bloch@ima.enst.fr

For neurological studies, brain images are currently a classical tool used in clinical routine and research. The most appropriate system to observe brain anatomy is tridimensional magnetic resonance imaging, and a major issue of image processing is to segment automatically cerebral structures. We present an original recognition method which is progressive and atlas-guided. As our process is sequential, we rely on objects that have been already recognized to perform the segmentation of objects which are *a priori* more and more difficult to obtain. To this aim, we take into account structural information processed as fuzzy spatial constraints; we use *a priori* radiometric, morphology and localization knowledge, and relative distance and direction relationships between objects. In this paper, we focus on the representation of such structural information.

**Keywords:** medical imaging, fuzzy pattern recognition, fuzzy mathematical morphology, fuzzy classification, fuzzy spatial relationships, fuzzy pattern matching, fuzzy fusion.

## 1. Introduction

Since anatomical brain imaging serves as a reference for clinical investigation and for functional imaging as well, segmentation of brain structures is of prime importance for many different applications: morphometry, pathology detection and measurement, diagnosis, surgery and radio-therapy planning, functional imaging, neuro-sciences and so forth.

A large body of literature has been devoted to brain image segmentation (see e.g. the syntheses in [1,9]). The use of artificial intelligence techniques in this domain concerns tissue classification, structure identification and diagnosis.

In magnetic resonance images (MRI), the classes that can be observed are, for the outer part of the brain, air, skin, muscle, fat and skull, and for the brain, white matter, grey matter and cerebro-spinal fluid. Although the radiometry of these classes can be described by statistical laws that significantly overlap, classifiers can separate the three main brain tissues. Both fuzzy clustering e.g. [8,15] and neural networks e.g. [6,16] have been widely used. Unfortunately, the recognition of internal structures remains difficult. For instance, the different grey nuclei which are constituted of grey matter cannot be distinguished using only radiometric information [12].

To face this problem, other methods make use of models. These models can be implicit like Physics-based deformable models e.g. [17,19] or explicit in atlas deformation techniques. Implicit models are often used when one specific structure of interest has to be detected, while atlas-based approaches can segment all structures but have to deal with difficult problems due to the anatomical variability. To find the atlas deformation that fits the image, the methods rely on homologous points [10], on surfaces [18], or on the whole volume [7,11].

In this paper, we propose a new atlas-based method for the recognition of brain internal structures in magnetic resonance images. Whereas existing atlas-based methods try to find a global deformation between the atlas and the image in order to identify anatomical objects, our method is sequential: one step aims at recognizing one single anatomical object and then refines the correspondence between the image and the atlas.

With the help of the atlas, the segmentation of an anatomical structure can be conditional to a region of interest with imprecise limits. A recognition step benefits also from knowledge that has been obtained during the previous steps and from relations between the object we look at and previously recognized objects. All this information is modeled with fuzzy sets in the image space. A two-stage fusion process leads to the selection of the radiometric mode of the object in the MRI acquisition and a final fusion process leads to the object recognition.

At each step, the correspondence between the surfaces of already recognized objects in the image and their equivalents in the atlas is found with a registration

* Current address: EPITA – Research and Development Laboratory – 14-16 rue Voltaire, 94276 Le Kremlin-Bicêtre cedex, France – Tel: +33 1 44 08 01 01, Fax: +33 1 44 08 01 99, E-mail: thierry.geraud@epita.fr

technique. A discrete deformation field is then inferred.

Section 2 gives an overview of our method and presents the different sub-steps of the recognition of one object. Section 3 details the construction of fuzzy sets from symbolic expressions and constitutes the core of this paper. Section 4 explains how to select the correct radiometric mode of the object in the MRI volume. At last, section 5 presents our results and concludes.

## 2. Method overview

To guide the recognition, we make use of an atlas which is neither a probabilistic atlas nor a mean atlas but a labeled image obtained from a MRI acquisition of a normal subject. A slice extracted from the atlas 3D volume is shown in Figure 1 (left); the right view shows the corresponding slice in the 3D MRI acquisition to be processed. Let us consider one step of the recognition process; during the preceding steps, several anatomical objects have been segmented and the correspondence that makes the image match the atlas has been computed according to the segmented objects. The current step can be described by seven sub-steps: the first five ones concern the recognition of another particular object and the two last sub-steps deal with the correspondence update to take into account this object.

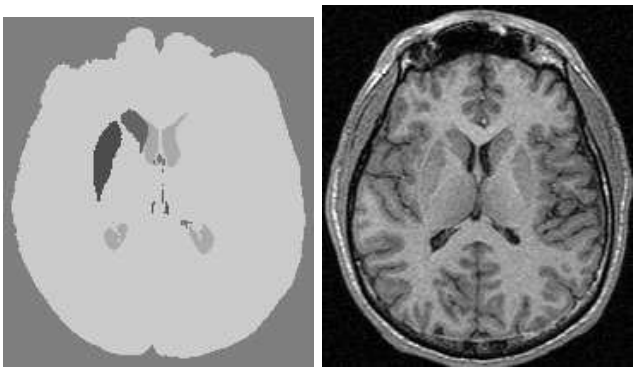

Figure 1. Slice extracted from the atlas and from the image.

*Sub-step 1* With the help of the correspondence field, the object definition given by the atlas is projected in the image.

*Sub-step 2* This information is dilated with a fuzzy morphological operator in order to define in the image a region of interest that should contain the object we look at (see section 3.1 for details). This region is an *a priori* information.

*Sub-step 3* Fuzzy classifications based on the radiometry are performed in the region of interest with different numbers of classes (see section 4.1 for details).

*Sub-step 4* Each piece of symbolic information that describes the object is expressed by a fuzzy set in the image space. It can be an *a priori* radiometric knowledge, a directional relationship with respect to an object that has already been recognized, and so forth. Fuzzy set construction is presented in section 3.

*Sub-step 5* A two-stage fuzzy fusion process combines the *a priori* information from sub-step 2 and symbolic knowledge from sub-step 4 including the *a priori* radiometric knowledge; we obtain two rough descriptions of the object we look at. With the help of similarity measures between these descriptions and the fuzzy sets resulting from the classifications of sub-step 3, the proper radiometric characteristic of the object in the image is selected (the selection process is explained in section 4.2). A final fusion process combines this radiometric information with all pieces of knowledge about the object excluding the *a priori* radiometric one; it leads to a fuzzy object description. A regularization followed by a binarization gives the object segmentation. This sub-step is illustrated in Figure 2.

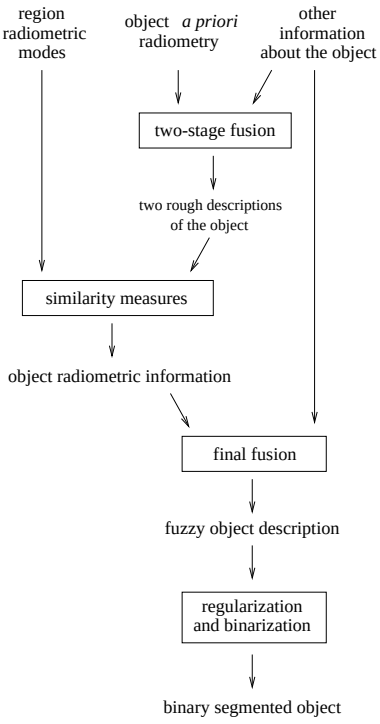


Figure 2. Sub-step 5: object recognition using information fusion.

*Sub-step 6* A discrete deformation to make the object definition provided by the atlas fit the segmented object is calculated with an elastic registration algorithm based on object surfaces.

*Sub-step 7* A new global volume correspondence is inferred from the set of surface deformations of the segmented objects.

## 3. From symbolic expressions to fuzzy sets

In the following, the image to be processed will be denoted by $I$, and a point (volume element) in this image, by $v(I)$. In anatomy, different pieces of knowledge about objects are given by symbolic expressions (substeps 2 and 4). In our method, these expressions are translated into fuzzy sets $\mu_{\text{knowledge}}$ in the image space:

$$\mu_{\text{knowledge}} : v(I) \mapsto \mu_{\text{knowledge}}(\, v(I)\,) \in [0,1].$$

We rely on fuzzy set theory for three reasons: information of various semantics can be expressed in this unique formalism, it helps us to model information imprecision and uncertainty, and the fusion process that leads to recognition can take benefits from a great number of operators [3].

### 3.1. A priori information

The projection in the image of the object definition given by the atlas gives us an indication about both the morphology and the localization of the object in the image. Although this information is made accurate with the help of the correspondence, we have to model the imprecision due to our correspondence model and to the variability of brain anatomy. It is done using a fuzzy morphological dilation [2]. The parameters of the dilation are set so that the resulting region of interest should contain the object we look at.

We use a spherical fuzzy structuring element which values have a radial symmetry. They are defined along the radius $r$ by a trapezoidal function $e(r)$ whose value is 1 for $r \leq r_k$ and 0 for $r > r_s$. These two parameters define the kernel and the support of the structuring element respectively and permit us to set the degree of fuzziness of the resulting region of interest.

A region of interest of $I$ is depicted in Figure 3 (top left). It represents an *a priori* information about both the morphology and the localization in $I$ of the object to be recognized. Let us denote by $\mu_{\text{apriori}}$ this information (here, it concerns the caudate nucleus).

### 3.2. Binary spatial constraint

For an object, spatial inclusion in another one ($O^{\text{in}}$) and spatial exclusions with other ones (indexed by $i$ and denoted by $O_i^{\text{out}}$) give a binary constraint $\mu_{\text{constraint}}$ that can be used in the fusion processes. Of course, such considerations only rely on objects $O$ that have already been recognized.

$$\mu_{\text{constraint}}(\, v(I)\,) = \begin{cases} 1 & \text{if } v(I) \in \{\, O^{\text{in}} \setminus \cup_i O_i^{\text{out}} \,\} \\ 0 & \text{elsewhere.} \end{cases}$$

Furthermore, this constraint ensures that the spatial inclusion of object volumes in the image reflects the one of the atlas.

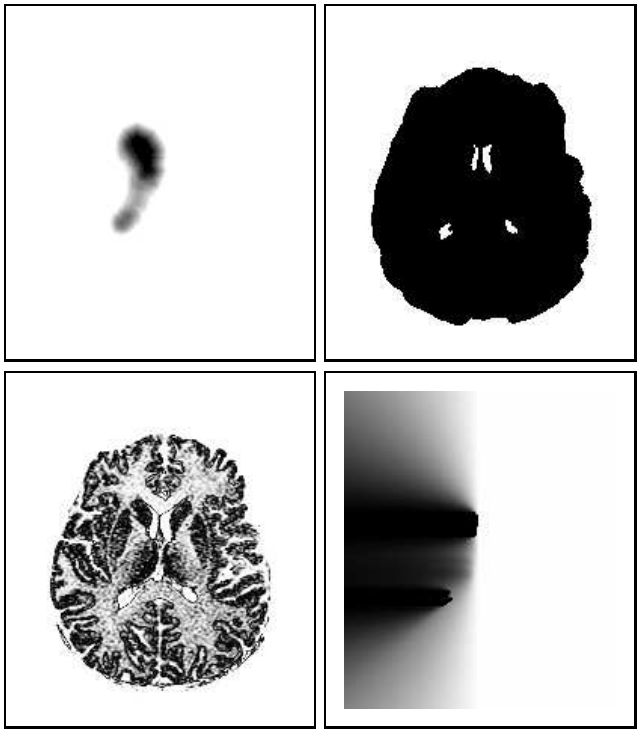

Figure 3. Information expressions in the image space.

At this step of the recognition process, three anatomical objects have been segmented: the brain and the two lateral ventricles (in top right view, respectively the black structure and its white holes). This figure depicts four equivalent slices extracted from fuzzy set images and concerning the recognition of the left caudate nucleus: the *a priori* information (top left), the localization constraint (top right), the *a priori* radiometric knowledge (bottom left) and a relative directional relationship (bottom right); white and black correspond respectively to minimal and maximal membership values to fuzzy sets.

In Figure 3 (top right), the binary set expresses that the object caudate nucleus belongs to the brain (black) but is distinct from both lateral ventricles (white components inside the brain).

### 3.3. Radiometric knowledge

A radiometric information first leads to a fuzzy set in the radiometry space $L = [0, 255]$:

$$\mu^{\text{L-radio}} : l \in L \mapsto \mu^{\text{L-radio}}(l) \in [0,1].$$

A representation in the image space is then constructed by assigning to each image point the membership of its grey-level in $L$. During the first steps, as the radiometric characteristics of brain tissues in the image are unknown, three fuzzy sets corresponding to dark, medium and light radiometries are built . The expressions "nuclei are made of grey matter", "grey matter is medium dark in MR acquisitions of type $T_1$" and "our image is a $T_1$-MRI" can also be used to describe the nuclei. For instance we have:

$$\mu_{\text{nucleus}}(\, v(I)\,) = \mu^{\text{L-medium dark}}(\, l(v(I))\,),$$

where $l(\,v(I)\,)$ denotes the radiometry of $(\,v(I)\,)$. The result is illustrated in Figure 3 (bottom left).

Once a nucleus is recognized, the radiometric characteristics of nuclei (mean $l_{\text{nucleus}}$ and variance $\sigma^2_{\text{nucleus}}$) are estimated and a more precise fuzzy set which signifies "has a radiometry of nuclei" is defined to be used in the following recognition steps. For that, we use a Gaussian law :

$$\mu^{\text{L-nucleus}}(l) = \exp\left(-|\,l - l_{\text{nucleus}}\,|^2 \,/\, 2\,\sigma^2_{\text{nucleus}}\right).$$

### 3.4. Relative distance

Distance information between anatomical objects are usually approximative. The distance between an object and a reference object is less than, or about, or more than $x$ millimeters, or between $x_1$ and $x_2$ millimeters. When there is a spatial inclusion or exclusion, we can say that an object is deep inside another or far outside. To translate these notions into the image space, we define a fuzzy set in the distance space $D = \mathbb{R}^+$:

$$\mu^{\text{D-distance}} : d \in D \mapsto \mu^{\text{D-distance}}(D) \in [0,1].$$

Then in the image space, we calculate a distance map $M$ to the reference object by a chamfer transform algorithm and we assign to each point in $I$ the membership of its distance map value as given by $\mu^{\text{D-distance}}$:

$$\mu_{\text{distance}}(\,v(I)\,) = \mu^{\text{D-distance}}(\,M(\,v(I)\,)\,).$$

### 3.5. Relative directional relationship

The vagueness of a directional relationship such as "the head of caudate nucleus is lateral to the head of the lateral ventricle" is modeled as described in [5]. In this technique, the resulting fuzzy set $\mu_{\text{direction}}$ corresponds to a morphological dilation of the reference object with a structuring element which is representative of the direction. This method gives natural results whatever the shape of the reference object is.

Figure 3 (bottom right) shows the dilated of the lateral ventricle which means "lateral to the lateral ventricle".

## 4. Selection of object radiometric mode

A major piece of information that permits to segment a brain structure using classical methods is its radiometric mode in the image. In our method, we perform several classifications with different numbers of classes in the region of interest that corresponds to the structure (sub-step 3). Then, the resulting classes are compared to a rough description of the structure given by a first information fusion, and the correct radiometric class is selected (sub-step 5).

### 4.1. Empiric classifications and their fuzzication

We have shown in [14] that the $k$-means algorithm gives more robust results when the number of classes is low and that its empirical use (for a given number of classes, we proceed to several classifications with random centroid initialization and we keep the best result) is required to guarantee the correctness of its results when the number of classes increases.

Performing the classification in a region of interest permits us to limit the number of classes and moreover to ensure that the object class can be found even if the radiometric law of the object is close to the ones of other nearby objects.

At first, the radiometry histogram of the fuzzy region of interest is calculated so that the contribution of each image point is weighted by its membership to the region. For each radiometry $l$, we have:

$$h(l) = \sum_{v(I),\, l(v(I))=l} \mu_{\text{apriori}}(\,v(I)\,)$$

With this histogram, automatic classifications are produced by an empiric use of the $k$-means algorithm with different numbers $n = 2..5$ of classes. Let us denote by $\omega_{i,n}$ the $i^{\text{th}}$ class with $n$ classes; its centroid and variance are:

$$c_{i,n} = \frac{\sum_{l\in\omega_{i,n}} h(l)\,l}{\sum_{l\in\omega_{i,n}} h(l)} \quad \text{and} \quad \sigma_{i,n} = \frac{\sum_{l\in\omega_{i,n}} h(l)\,l^2}{\sum_{l\in\omega_{i,n}} h(l)} - c^2_{i,n}.$$

Each resulting class is then translated into a fuzzy set in the image space to take into account the noise and imprecision of MR images:

$$\mu_{\text{class}\,i,n}(\,v(I)\,) = \exp\left(-|\,l(\,v(I)\,) - c_{i,n}\,|^2 \,/\, 2\,\sigma^2_{i,n}\right).$$

Figure 4 shows the resulting fuzzy sets. Each fuzzy set is a candidate for the object radiometric mode.

### 4.2. Radiometric mode selection

To find out the object radiometric mode, we perform a two-stage selection.

- First, we select for each classification the most appropriate candidate mode $\mu_{\text{class}\,i_n,n}$. For that, we calculate a fuzzy pattern similarity measure [4] in the image space between two fuzzy sets $\mu_{\text{object}\,i,n}$ and $\mu_{\text{description1}}$. The former is constructed from a class mode:

  $$\mu_{\text{object}\,i,n} = \min\left(\,\mu_{\text{class}\,i,n},\, \mu_{\text{apriori}}\,\right),$$

  and the latter is an object rough description which is radiometrically discriminant (depicted in the top left view in Figure 5):

  $$\mu_{\text{description1}} = \min\left(\,\mu_{\text{radiometry}},\, \mu_{\text{apriori}}\,\right).$$

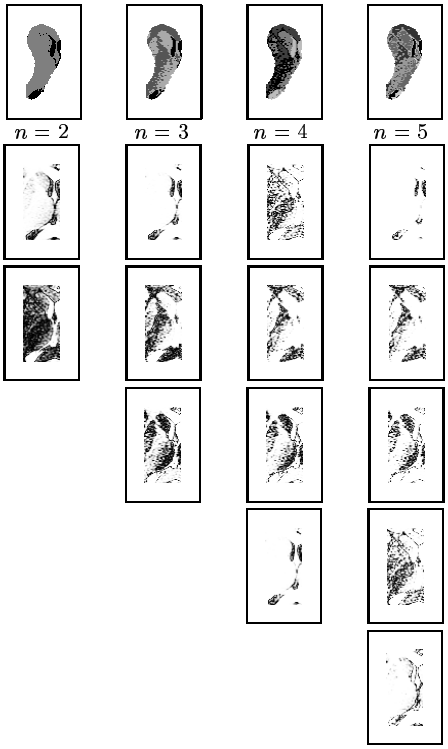


Figure 4. Radiometric classes of a region of interest.

The first line shows the results of an empiric use of the $k$-means algorithm processed on a region of interest histogram with different number $n$ of classes. The fuzzification of the classes is depicted in column below the rough classification. For the caudate nucleus, the best radiometric fuzzy set is obtained for $n = 3$ (second column) and $i = 3$ (last raw of this column).

The similarity measure we use represents the fraction of the pattern intersection by the pattern union:

$$\frac{\sum_{v(I)} \min(\,\mu_{\text{object } i,n}(\,v(I)\,),\ \mu_{\text{description1}}(\,v(I)\,)\,)}{\sum_{v(I)} \max(\,\mu_{\text{object } i,n}(\,v(I)\,),\ \mu_{\text{description1}}(\,v(I)\,)\,)}.$$

- Then, we select the best radiometric mode $\mu_{\text{class } i_{n_s},n_s}$ over the remaining candidates. For this final selection, the similarity measure is applied between each fuzzy set $\mu_{\text{object } i_n,n}$ and a second object description which is built, for the caudate nucleus, by fusing the *a priori* information, the binary constraint, and the directional relationship. This second description, depicted in Figure 5 (top right), provides the expected localisation and morphology of the object.

### *4.3. End of a recognition step*

A final fusion process combines *a priori* information, symbolic information and the selected radiometric information, and gives the fuzzy object depicted in Figure 5 (bottom left). Fuzzy fusion operators used in each fusion process vary from one step to another in order to take into account both the specificity of each anatomical object and the evolution of knowledge. A regularization

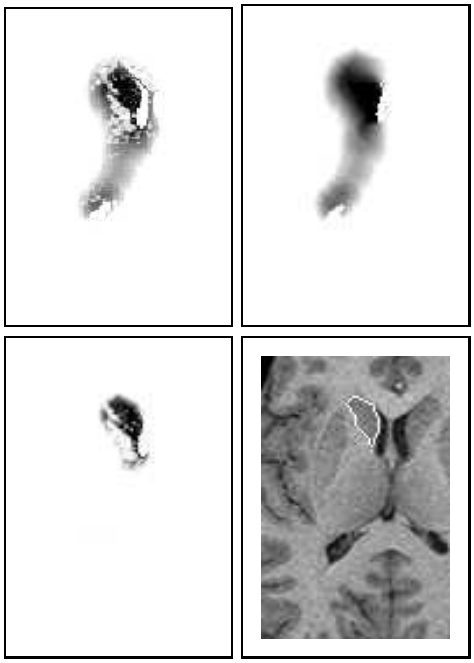

Figure 5. Radiometric mode selection, fusion and segmentation.

The information based on radiometry knowledge (top left) is compared to each fuzzy class resulting of a classification (for each column in figure 4, we get a candidate class). The information which is representative of the object localization and morphology (top right) permits to find the correct radiometric class among the different candidates. A fusion process gives a fuzzy object (bottom left) and the segmented object is deduced. Its boundary is depicted in white, superimposed on the MRI (bottom right).

followed by a binarization leads to the object segmentation (Figure 5, bottom right).

A discrete deformation to make the object definition provided by the atlas fit the segmented object is calculated with an elastic registration algorithm based on surfaces (sub-step 6). Then, a new global volume correspondence is inferred from the set of object deformations (sub-step 7). For that, we have proposed a discrete method which relies on a simple mathematical model (the Laplacian of the deformation field is null) and which resolution is iterative and local to areas bounded by object surfaces [14].

## 5. Results and conclusion

The recognition procedure is initialized by a segmentation of the brain using mathematical morphology operators [13]. Then, we perform the recognition of lateral ventricles, caudate nuclei, putamen, and third and fourth ventricles (that have only been segmented until now with dedicated approaches). The recognition sequence reflects that we process in the first recognition steps the objects that can be easily segmented and the location and morphology of which are of prime importance for anatomy description. The objects which are

difficult to obtain are processed in the following steps and, with the help of pieces of information relative to the former objects and of more precise pieces of knowledge, their segmentation succeeds.

Figure 6 shows these objects as defined in the atlas and as recognized in an MR image with our method. They are correctly segmented although the size, the location and the morphology of these objects in the image significantly differ from their definitions in the atlas.

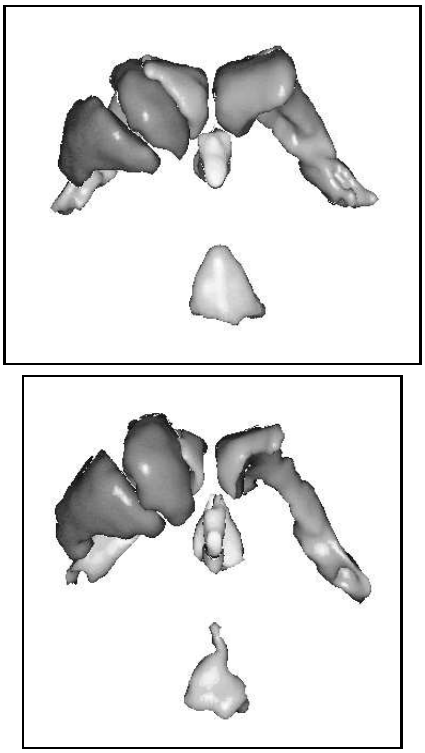

Figure 6. Recognition results.

The upper view represents six objects from the atlas: lateral ventricles (medium grey), third and fourth ventricles (light grey), caudate nucleus and putamen (dark grey). The lower view represents the equivalent objects recognizied from a MRI acquisition.

We have presented an original recognition method which is atlas-guided and progressive, and which takes into account structural information. A main feature of our method is that anatomical knowledge is directly expressed in the image space by the mean of fuzzy sets while taking advantage of objects that have already been recognized.

## References


[1] J.C. Bezdek, L.O. Hall, and L.P. Clarke, *Review of MR image segmentation techniques using pattern recognition*, Medical Physics, 20:4 (1993) 1033-1048.

[2] I. Bloch and H. Maître, *Fuzzy mathematical morphologies: a comparative study*, Pattern Recognition, 28:9 (1995) 1341–1387.

[3] I. Bloch, *Information combination operators for data fusion: a comparative review with classification*, IEEE Trans. on Systems, Man, and Cybernetics, 26:1 (1996) 52-67.

[4] I. Bloch, *On fuzzy distances and their use in image processing under imprecision*, Pattern Recognition, (1999), to appear.

[5] I. Bloch, Fuzzy relative position between objects in image processing: a morphological approach, IEEE Trans. on Pattern Analysis and Machine Intelligence, (1999), to appear.

[6] K. Cheng, J. Lin, and C. Mao, *The application of competitive hopfield neural network to medical image segmentation*, IEEE Trans. on Medical Imaging, 15 (1996) 560-567.

[7] G.E. Christensen, R.D. Rabbitt, and M.I. Miller, *3D brain mapping using a deformable neuroanatomy*, Phys. Med. Biol., 39 (1994) 609-618.

[8] M.C. Clark, L.O. Hall, D.B. Goldgof, L.P. Clarke, R.P. Velthuizen, and M.S. Silbiger, *MRI segmentation using fuzzy clustering techniques*, IEEE Engineering in Medicine and Biology, 13:5 (1994) 730-742.

[9] L.P. Clarke, R.P. Velthuizen, M.A. Camacho, J.J. Heine, M. Vaidyanathan, L.O. Hall, R.W. Thatcher, and M.L. Silbiger, *MRI segmentation: methods and applications*, Journal of Magnetic Resonance Imaging, 13:3 (1995) 343-368.

[10] A.C. Evans, D.L. Collins, and C.J. Holmes, *Computational approaches to quantifying human neuroanatomical variability*, in: Brain Mapping – The Methods. A.W. Toga and J.C. Mazziotta Editors, Academic Press, 1996, pp. 343-361.

[11] J.C. Gee, L. LeBriquer, C. Barillot, and D.R. Haynor, *Probabilistic matching of brain images*, in: Y. Bizais, C. Barillot, and R. DiPaola, editors, Computational Imaging and Vision: Information Processing in Medical Imaging, vol. 2432, Kluwer Academic, 1995, pp. 113-126.

[12] T. Géraud, J.F. Mangin, I. Bloch and H. Maître, *Segmenting internal structures in 3D MR images of the brain by Markovian relaxation on a watershed based adjacency graph*, in: IEEE Int. Conf. on Image Processing, Washington DC, U.S.A., vol. 3, 1995, pp. 548-551.

[13] T. Géraud, I. Bloch and H. Maître, *Robust radiometric parameter estimation and automatic morphological segmentation of brain internal structures in 3D MR images*, in: Int. Conf. on Computer Assisted Radiology, Paris, France, 1995, p. 1007.

[14] T. Géraud, *Segmentation des structures internes du cerveau en imagerie par résonance magnétique tridimensionnelle*, Ph.D. Thesis (in french), Signal and Image Processing Department, Ecole Nationale Supérieure des Télécommunications, Paris, France, 1998.

[15] D. Pham, J.L. Prince, C. Xu, and A.P. Dagher, *An automated technique for statistical characterization of brain tissues in magnetic resonance imaging*, Int. Journal of Pattern Recognition and Artificial Intelligence, 11:8 (1997) 1189-1211.

[16] W.E. Reddick, J.O. Glass, E.N. Cook, T.D. Elkin, and J. Deaton, *Automated segmentation and classification of multispectral magnetic resonance images of brain using artificial neural networks*, IEEE Trans. on Medical Imaging, 16:6 (1987) 911-918.

[17] L.H. Staib, A. Chakraborty, and J.S. Duncan, *An integrated approach for locating neuroanatomical structure from MRI*, Int. Journal of Pattern Recognition and Artificial Intelligence, 11:8 (1997) 1247-1269.

[18] P.M. Thompson and A.W. Toga, *A surface-based technique for warping three-dimensional images of the brain*, IEEE Trans. on Medical Imaging, 15:4 (1996) 402-417.

[19] P.E. Undrill, K. Delibasis, and G.G. Cameron, *An application of genetic algorithms to geometric model-guided interpretation of brain anatomy*, Pattern Recognition, 30:2 (1997) 217-227.